

# Possible Quantum Critical Region tuned by the Disorder and Pauli-Blocking Effects

A. Kwang-Hua Chu

Department of Physics, Xinjiang University,  
Urumqi 830046, PR China

## Abstract

Based on the acoustic analog, we investigate both of the effects : disorder and (Pauli-blocking) interaction to the possible localization in electron gases by using the quantum discrete kinetic model. Effects of the disorder (or free-orientation :  $\theta$  which is related to the relative direction of scattering of particles w.r.t. to the normal of the propagating plane-wave front) which is introduced into the Ühling-Uhlenbeck equations together with those of the Pauli-blocking are presented. We obtain the possible phase diagram (related to the strength of disorders and the mean free path) which resembles qualitatively that proposed by Abrahams<sup>1</sup>.

PACS : 71.10.Hf; 71.30.+h; 73.43.Nq; 73.20.Jc; 73.20.Fz

An intriguing aspect of quantum mechanics is that even at absolute zero temperature quantum fluctuations prevail in a system, whereas all thermal fluctuations are frozen out. These quantum fluctuations are able to induce a macroscopic phase transition in the ground state of a many-body system, when the ratio of two competing terms in the underlying Hamiltonian is varied across a critical value [1-4]. The instability of the quantum critical behavior with respect to (w.r.t.) the disorder can be interpreted as a signal for phenomena of localization. Recently some of the new developments in the localization problem [5] have become a major theme in the condense matter research. One example is the strongly-interacting electron (non-Fermi) liquid with different strengths of disorder [6]. Interesting issues are the quantum phase transition (QPT) and quantum critical point (QCP). Both effects of disorder and interaction are closely relevant to the weak and strong localization [8, 9]. They are then related to the metal-insulator transition in two-dimensions (2D). Although most of theories proposed before are based on the Fermi liquid behavior, new insights could be obtained considering the possible analogy with superconducting transition which might be related to the bosonic system [2-3].

In the last two decades a variety of metals have been discovered which display thermodynamic and transport properties at low temperatures which are fundamentally different from those of the usual metallic systems which are well described by the Landau Fermi-liquid theory. The resistivity in a variety of high mobility 2D electron/hole systems is seen experimentally to exhibit a number of interesting anomalies that don't as yet have an adequate theoretical understanding. Note that, at sufficiently low electron densities, an ideal two-dimensional electron systems becomes strongly correlated, because the kinetic energy is overpowered by energy of electron-electron interactions (exchange and correlation energy). The interaction strength is normally

described by the Wigner-Seitz radius,  $r_s = 1/(\pi n_s)^{1/2} a_B$  (where  $n_s$  is the electron density and  $a_B$  is the effective Bohr radius in semiconductor). Till now, for rather large  $r_s$  ( $\gg 1$ ) and together with disorder, the nature of this metal-insulator transition (MIT) remains the subject of ongoing debate [6,8-9].

Motivated by the analogy between electrons in periodic or disordered metals and waves in classical acoustical systems [10-12] an investigation for observing possible QCP in MIT or relevant localization [8] using the quantum discrete kinetic model [13-14] was performed and will be presented here. In present approach the Ühling-Uhlenbeck collision term [13] which could describe the collision of a gas of dilute hard-sphere Fermi- or Bose-particles by tuning a parameter  $\gamma$  : a Pauli-blocking factor (or  $\gamma f$  with  $f$  being a normalized (continuous) distribution function giving the number of particles per cell) is adopted together with a disorder or free-orientation ( $\theta$  which is related to the relative direction of scattering of particles w.r.t. to the normal of the propagating plane-wave front) into the quantum discrete kinetic model which can be used to obtain dispersion relations of (plane) sound waves propagating in quantum gases. We then study the quantum critical behavior based on the acoustical analog [15-17] which has been verified before. The possible phase diagram for MIT and/or resistance(or disorder)-scattering amplitude curves (as the temperature is decreased ) we obtained resemble qualitatively those proposed in [5] (cf Fig. 4 therein). The non-Fermi liquid behavior was also clearly illustrated here.

We firstly introduce the concept of acoustical analog [15] in brief. In a mesoscopic system, where the sample size is smaller than the mean free path for an elastic scattering, it is satisfactory for a one-electron model to solve the time-independent Schrödinger equation :  $-(\hbar^2/2m)\nabla^2\psi + V'(\vec{r})\psi = E\psi$  or (after dividing by  $-\hbar^2/2m$ )  $\nabla^2\psi + [q^2 - V(\vec{r})]\psi = 0$ , where  $q$  is an (energy) eigenvalue parameter, which for the quantum-mechanic system is  $\sqrt{2mE/\hbar^2}$ . Meanwhile, the equation for classical (scalar) waves is  $\nabla^2\psi - (\partial^2\psi/c^2 \partial t^2) = 0$  or (after applying a Fourier transform in time and contriving a system where  $c$  (the wave speed) varies with position  $\vec{r}$ )  $\nabla^2\psi + [q^2 - V(\vec{r})]\psi = 0$ , here, the eigenvalue parameter  $q$  is  $\omega/c_0$ , where  $\omega$  is a natural frequency and  $c_0$  is a reference wave speed. Comparing the time dependencies one gets the quantum and classical relation  $E = \hbar\omega$  [15-17].

We assume that the gas is composed of identical hard-sphere particles of the same mass [13, 14, 18]. The velocities of these particles are restricted to, e.g., :  $\mathbf{u}_1, \mathbf{u}_2, \dots, \mathbf{u}_p$ ,  $p$  is a finite positive integer. The discrete number densities of particles are denoted by  $N_i(\mathbf{x}, t)$  associated with the velocities  $\mathbf{u}_i$  at point  $\mathbf{x}$  and time  $t$ . If only nonlinear binary collisions and the evolution of  $N_i$  are considered, we have

$$\frac{\partial N_i}{\partial t} + \mathbf{u}_i \cdot \nabla N_i = F_i \equiv \frac{1}{2} \sum_{j,k,l} (A_{kl}^{ij} N_k N_l - A_{ij}^{kl} N_i N_j), \quad i \in \Lambda = \{1, \dots, p\}, \quad (1)$$

where  $(i, j)$  and  $(k, l)$  ( $i \neq j$  or  $k \neq l$ ) are admissible sets of collisions [13-14,16-18] Here, the summation is taken over all  $j, k, l \in \Lambda$ , where  $A_{kl}^{ij}$  are nonnegative constants satisfying [13-14,18]  $A_{kl}^{ji} = A_{kl}^{ij} = A_{lk}^{ij}$ ,  $A_{kl}^{ij}(\mathbf{u}_i + \mathbf{u}_j - \mathbf{u}_k - \mathbf{u}_l) = 0$ , and  $A_{kl}^{ij} = A_{ij}^{kl}$ . The conditions defined for the discrete velocities above require that there are elastic, binary collisions, such that momentum and energy are preserved, i.e.,  $\mathbf{u}_i + \mathbf{u}_j = \mathbf{u}_k + \mathbf{u}_l$ ,  $|\mathbf{u}_i|^2 + |\mathbf{u}_j|^2 = |\mathbf{u}_k|^2 + |\mathbf{u}_l|^2$ , are possible for  $1 \leq i, j, k, l \leq p$ . We note that, the summation of  $N_i$  ( $\sum_i N_i$ ) : the total discrete number density here is related to the macroscopic density :  $\rho (= m_p \sum_i N_i)$ , where  $m_p$  is the mass of the particle

[18].

Together with the introducing of the Ühling-Uhlenbeck collision term [13] :  $F_i = \sum_{j,k,l} A_{kl}^{ij} [N_k N_l (1 + \gamma N_i)(1 + \gamma N_j) - N_i N_j (1 + \gamma N_k)(1 + \gamma N_l)]$ , into equation (1), for  $\gamma < 0$  (normally,  $\gamma = -1$ ), we can then obtain a quantum discrete kinetic equation for a gas of Fermi-particles; while for  $\gamma > 0$  (normally,  $\gamma = 1$ ) we obtain one for a gas of Bose-particles, and for  $\gamma = 0$  we recover the equation (1).

Considering binary collisions only, from equation above, the model of quantum discrete kinetic equation for Fermi or Bose gases proposed in [13-14] is then a system of  $2n(= p)$  semilinear partial differential equations of the hyperbolic type :

$$\begin{aligned} \frac{\partial}{\partial t} N_i + \mathbf{v}_i \cdot \frac{\partial}{\partial \mathbf{x}} N_i = \frac{cS}{n} \sum_{j=1}^{2n} N_j N_{j+n} (1 + \gamma N_{j+1})(1 + \gamma N_{j+n+1}) - \\ 2cS N_i N_{i+n} (1 + \gamma N_{i+1})(1 + \gamma N_{i+n+1}), \quad i = 1, \dots, 2n, \end{aligned} \quad (2)$$

where  $N_i = N_{i+2n}$  are unknown functions, and  $\mathbf{v}_i = c(\cos[\theta + (i-1)\pi/n], \sin[\theta + (i-1)\pi/n])$ ;  $c$  is a reference velocity modulus and the same order of magnitude as that ( $c$ , the sound speed in the absence of scatters) used in Ref. 9,  $\theta$  is the orientation starting from the positive  $x$ -axis to the  $u_1$  direction and could be thought of as a parameter for introducing a *disorder* [15, 10, 16, 17, 20],  $S$  is an effective collision cross-section for the collision system.

Since passage of the sound wave will cause a small departure from an equilibrium state and result in energy loss owing to internal friction and heat conduction, we linearize above equations around a uniform equilibrium state (particles' number density :  $N_0$ ) by setting  $N_i(t, x) = N_0 (1 + P_i(t, x))$ , where  $P_i$  is a small perturbation. After some similar manipulations as mentioned in [14-17], with  $B = \gamma N_0 < 0$  [13, 14], which gives or defines the (proportional) contribution from the Fermi gases (if  $\gamma < 0$ , e.g.,  $\gamma = -1$ ), we then have

$$\left[ \frac{\partial^2}{\partial t^2} + c^2 \cos^2 \left[ \theta + \frac{(m-1)\pi}{n} \right] \frac{\partial^2}{\partial x^2} + 4cSN_0(1+B) \frac{\partial}{\partial t} \right] D_m = \frac{4cSN_0(1+B)}{n} \sum_{k=1}^n \frac{\partial}{\partial t} D_k, \quad (3)$$

where  $D_m = (P_m + P_{m+n})/2$ ,  $m = 1, \dots, n$ , since  $D_1 = D_m$  for  $1 = m \pmod{2n}$ .

We are ready to look for the solutions in the form of plane wave  $D_m = a_m \exp i(kx - \omega t)$ , ( $m = 1, \dots, n$ ), with  $\omega = \omega(k)$ . This is related to the dispersion relations of 1D (forced) plane wave propagation in Fermi gases. So we have

$$\left( 1 + ih(1+B) - 2\lambda^2 \cos^2 \left[ \theta + \frac{(m-1)\pi}{n} \right] \right) a_m - \frac{ih(1+B)}{n} \sum_{k=1}^n a_k = 0, \quad m = 1, \dots, n, \quad (4)$$

where

$$\lambda = kc/(\sqrt{2}\omega), \quad h = 4cSN_0/\omega \quad \propto \quad 1/K_n,$$

where  $h$  is the rarefaction parameter of the gas;  $K_n$  is the Knudsen number which is defined as the ratio of the mean free path of gases to the wave length of the plane (sound) wave.

We can obtain the complex spectra ( $\lambda = \lambda_r + i \lambda_i$ ;  $\lambda_r = k_r c/(\sqrt{2}\omega)$ ): sound dispersion, a relative measure of the sound or phase speed;  $\lambda_i = k_i c/(\sqrt{2}\omega)$  : sound attenuation or absorption) from the complex polynomial equation above. Here,  $B$  could be related to the occupation number of

different-statistic particles of gases To examine the critical region possibly tuned by the Pauli-blocking measure  $B = \gamma N_0$  and the disorder  $\theta$ , as evidenced from our preliminary results :  $\lambda_i = 0$  for cases of  $B = -1$  or  $\theta = \pi/4$  [17], we firstly check those spectra near  $\theta = 0$ , say,  $\theta = 0.005$  and  $\theta = \pi/4 \approx 0.7854$ , say,  $\theta = 0.78535$  for a  $B$ -sweep ( $B$  decreases from 1 to -1). We plot them into figures 1, 2, respectively. Note that, as the disorder or free-orientation  $\theta$  is not zero, there will be two kinds of propagation of the disturbance wave : sound and diffusion modes [16-17,19-20]. The latter (anomalous) mode has been reported in Boltzmann gases [19,21] and is related to the propagation of entropy wave which is not used in the acoustical analog here. The absence of (further) diffusion (or maximum absorption) for the sound mode at certain state ( $h$ , corresponding to the inverse of energy  $E$ ; cf. Refs. 11 or 15) is classified as a localized state [11,15,17]. The state of decreasing  $h$  corresponds to that of  $T$  (absolute temperature) decreasing as the mean free path is increasing (density or pressure decreasing).

We can observe the max.  $\lambda_i$  (absorption of sound mode, relevant to the localization length according to the acoustical analog [15,17]) drop to around four orders of magnitude from  $\theta = 0.005$  to  $0.78535$ ! This is a clear demonstration of the effect of disorder. Meanwhile, once the Pauli-blocking measure ( $B$ ) increases or decreases from zero (Boltzmann gases), the latter (Fermi gases :  $B < 0$ ) shows opposite trend compared to that of the former (Bose gases :  $B > 0$ ) considering the shift of the max.  $\lambda_i$  state ( $\delta h$ ).  $\delta h > 0$  is for Fermi gases ( $|B|$  increasing), and the reverse ( $\delta h < 0$ ) is for Bose gases ( $B$  increasing)! This illustrates partly the electron-electron interaction effect (through the Pauli exclusion principle). These results will be crucial for further obtaining the phase diagram (flow to metallic or insulating state as the density or temperature is decreased) tuned by both disorder and the (electron-electron) interaction below. Here,  $B = -1$  or  $\theta = 0, \pi/4$  might be fixed points commented in [22].

To check what happens when the temperature is decreased (or the density or  $h$  is decreased) to near  $T = 0$ , we collect all the data based on the acoustical analog from the dispersion relations (especially the absorption of sound mode) we calculated for ranges in different degrees of disorder (here,  $\theta$  is up to  $\pi/4$  considering single-particle scattering and binary collisions; in fact, effects of  $\theta$  are symmetric w.r.t.  $\theta = \pi/4$  for  $0 \leq \theta \leq \pi/2$  [17]) and Pauli-blocking measure. After that, we plot the possible phase diagram for the (dimensionless) conductivity vs. the absolute (dimensionless) temperature into Fig. 3 (for different  $B$ s :  $B = -0.9, -0.7, -0.5, -0.3, 0.1$ ). Here, MFP is the mean free path and the temperature vs. MFP relations could be traced from [23] (cf. Fig. 3 therein). Note that, the resistivity or resistance is proportional to the strength of disorder in 2D (in the sense that for weak disorder it is given by  $1/(k_F l)$ , in units of  $\hbar/e^2$ ;  $k_F$  is the Fermi wave number,  $l$  is the mean free path associated with the usual Drude conductivity) [5]. This figure shows that as the temperature decreases to a rather low value, the resistivity (or strength of disorder) will decrease sharply (at least for Bose or Fermi gases). There is no doubt that this result resembles qualitatively that proposed before [5,24-25].

To know the detailed effects of electron-electron interactions (tuned by  $B$ s here), we plot the corresponding figure as shown in Fig. 4. Each contour line (flow path relevant to a specific  $B$  tuned by the disorder) represents the behavior when  $T$  is decreased, and different (flow) lines represent different values of scattering amplitude ( $S_b \propto K_n$  or  $r_s$ ). Interesting results are (i) there seems to be a quantum phase transition boundary (interface or regime) for bosonic-like

particles ( $B > 0$ ) which resembles that of high-temperature superconducting phase transition due to doping if we treat the strength of disorder to be equivalent to the doping amount! (ii) as evidenced in the top part of this plot for the Bose gases (near QCPs for smaller resistivity together with rather large arrows), it confirms Larkin's comment (cf page 793 in [2] by Larkin) : both Bose and Fermi approaches are important for the (QP) transition; Bose approach is more useful in a small region close to the transition!

To make sure we already recover previous proposed results (possible renormalization group (RG) flows for disorder plus interactions or scattering amplitude-resistance curves or suggested phase diagram tuned by  $r_s$  and disorder, cf. [5] or [24-25]), we summarize our results by illustrating them into a 3D plot as demonstrated in Fig. 5. Crossover lines separate those flows which begin at  $T > 0$  at small resistance (disorder or the inverse of conductance :  $1/G$ ) and flow initially, as the temperature is lowered, toward larger resistance but then are repelled by the fixed point and flow to large  $S_b$  (or  $r_s$ ) and large  $G$  (metallic behavior) from those which begin at larger disorder (or smaller  $G$ ) and flow toward very-large disorder (insulating behavior). Again, this result resembles that proposed before (cf. [5] or [24-25] therein). Note that, this flow is also similar to those in [24-25] (e.g., cf. Fig. 41 by Aoki [24]). Meanwhile, as expected before, at  $T = 0$ , a 2D system would become a Wigner crystal phase at  $r_s \geq 37$  [26]. This lies possibly near or above the rather large  $S_b$  position with zero strength of disorder in our illustrations. Possible QCPs happen around  $S_b \sim 80$  for  $B = 0.85$  but  $S_b \sim 10$  for  $B = 0.1$ .

To conclude in brief, our illustrations here, although are based on the acoustical analog of our quantum discrete kinetic calculations, can indeed show the non-Fermi liquid and quantum critical behavior for the metal-insulator transition in 2D [27-31] as the temperature is decreased to rather low values.

## References

- [1] J. Custers, *et al*, Nature **424**, 524 (2003). J. Hertz, Phys. Rev. B **14**, 1165 (1976). A.J. Millis, Physica B **312-313**, 1 (2002).
- [2] A.M. Goldman, Physica E **18**, 1 (2003). A. Larkin, Ann. Phys. (Leipzig) **8**, 785 (1999). M.P.A. Fisher, Phys. Rev. Lett. **65**, 923 (1990).
- [3] M. Greiner, *et al*, Nature **415**, 39 (2002).
- [4] G. Modugno, *et al*, Science **297**, 2240 (2002). K.E. Strecker, G.B. Partridge, and R.G. Hulet, Phys. Rev. Lett. **91**, 080406 (2003). C.A. Regal and D.S. Jin, Phys. Rev. Lett. **90**, 230404 (2003).
- [5] E. Abrahams, Physica E **3**, 69 (1998).
- [6] E. Abrahams, S.V. Kravchenko, and M.P. Sarachik, Rev. Mod. Phys. **73**, 251 (2001).
- [7] L.D. Landau, Sov. Phys. JETP **5**, 101 (1957). C.M. Varma, Z. Nussinov, and W. van Saarloos, Phys. Rep. **361**, 267 (2002).
- [8] N.F. Mott, Rep. Prog. Phys. **47**, 909 (1984). P.W. Anderson, Comments Solid Stat. Phys. **2**, 193 (1970).
- [9] A.M. Finkel'stein, Z. Physik B **56**, 189 (1984). B.L. Altshuler, D.L. Maslov, and V.M. Pudalov, Physica E **9**, 209 (2001). A.P. Taylor and A. MacKinnon, J. Phys. Condens. Matter **14**, 8663 (2002). V. Dobrosavljević, *et al*, Phys. Rev. Lett. **79**, 455 (1997). C. Castellani, *et al*, Phys. Rev. B **30**, 1596 (1984).

- [10] P.W. Anderson, Phys. Rev. **109** 1492 (1958). A. Figotin and A. Klein, Commun. Math. Phys. **180** 439 (1996).
- [11] T.R. Kirkpatrick, Phys. Rev. B **31** 5746 (1985).
- [12] S. John, Phys. Today **44** 32 (1991). A. Klein and A. Kohn, Mathematical Physics, Analysis and Geometry **4** 97 (2001). M. Aizenman, J.H. Schenker, R.M. Friedrich, and D. Hundertmark, Commun. Math. Phys. **224** 219 (2001).
- [13] V.V. Vedenyapin, I.V. Mingalev, and O.V. Mingalev, Russian Academy of Sciences Sbornik Mathematics **80** 271 (1995).
- [14] A. K.-H. Chu, J. Phys. B At. Mol. Opt. Phys. **34** L711 (2001). A. K.-H. Chu, Phy. Scripta (to be appeared, 2004).
- [15] J.D. Maynard, Rev. Mod. Phys. **73** 401 (2001).
- [16] K.-H. W. Chu, J. Phys. A Math. and General **34**, L673 (2001). W. K.-H. Chu, Appl. Math. Lett. **14** 275 (2001).
- [17] A. K.-H. Chu, Phys. Rev. E **66** 047106 (2002).
- [18] T. Platkowski and R. Illner, SIAM Rev. **30** 213 (1988). N. Bellomo and T. Gustafsson, Rev. Math. Phys. **3** 137 (1991).
- [19] A. K.-H. Chu, Eur. Phys. J. B **10** 1 (1999).
- [20] A. K.-H. Chu, Preprint (2002). A. K.-H. Chu, (in Press, 2003).
- [21] R.J. Jr. Mason, in *Rarefied Gas Dynamics*, edited by J.H. de Leeuw (Academic Press, New York, 1965), vol. 1, p. 48.
- [22] P.W. Anderson, Physica B **318**, 28 (2002).
- [23] D. Einzel and J.M. Parpia, J. Low Temp. Phys. **109** 1 (1997).
- [24] H. Aoki, Rep. Prog. Phys. **50**, 655 (1987).
- [25] D.V. Shopova and D.I. Uzunov, Phys. Rep. **379**, 1 (2003).
- [26] E. Wigner, Phys. Rev. **46**, 1002 (1934). B. Tanatar and D.M. Ceperley, Phys. Rev. B **39**, 5005 (1989).
- [27] A. Punnoose and A.M. Finkel'stein, Phys. Rev. Lett. **88**, 016802 (2002). M. Hilke, Phys. Rev. Lett. **91**, 226403 (2003).
- [28] V.M. Pudalov, *et al*, Phys. Rev. Lett. **91**, 126403 (2003). A.A. Shashkin, *et al*, Phys. Rev. Lett. **86**, 086801 (2001).
- [29] Y.Y. Proskuryakov, *et al*, Phys. Rev. Lett. **89**, 076406 (2002). R.J. Bell, Rep. Prog. Phys. **35**, 1315 (1972).
- [30] R. Shankar, Rev. Mod. Phys. **66**, 199 (1994). S. Sachdev, Quantum Phase Transitions (Cambridge Univ. Press, 1999). T. Chakraborty and V.M. Apalkov, Adv. Phys. **52**, 455 (2003). A.F. Hebard and M.A. Paalanen, Phys. Rev. Lett. **65**, 927 (1990).
- [31] M.P.A. Fisher and D.H. Lee, Phys. Rev. B **39**, 2756 (1989).

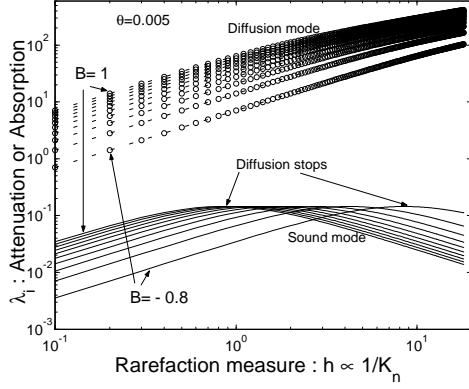


Fig. 1 Variations of the smaller (Sound mode) and larger (Diffusion mode [19,21])  $\lambda_i$  w.r.t.  $h$  for the same disorder :  $\theta = 0.005$  in different Pauli-blocking measures ( $B > 0$  corresponds to Bose gases). The maximum absorption states for sound modes correspond to possible localized states as the diffusion stops.  $B$  decreases from 1 (the highest) to  $-1$  with the decrement being  $-0.2$ .  $\lambda_i = 0$  as  $B = -1$ .  $h = 4cSN_0/\omega$ .  $N_0$  is the number density and  $S$  is the effective collision cross-section.

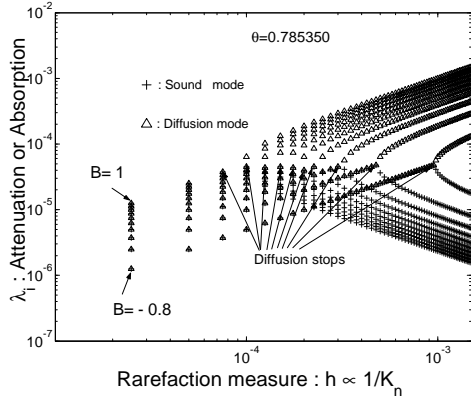


Fig. 2 Pauli-blocking ( $B$ ) effects on the absorption  $\lambda_i$ . (Note that the localization length  $\propto 1/\lambda_i$ , cf. [11,16-17]. The energy  $E$  (relevant to the illustration of localized states in [11]) corresponds to  $\hbar\omega$  [15-16].  $E \propto 1/h$  once  $cSN_0$  is fixed.)  $B$  decreases from 1 (the highest) to  $-1$  with the decrement being  $-0.2$ . Bose and Fermi gases are in opposite trend for the same increment  $|B| = 0.2$ .  $\theta = 0.78535$  and  $\lambda_i = 0$  as  $\theta = \pi/4 \approx 0.7854$ .

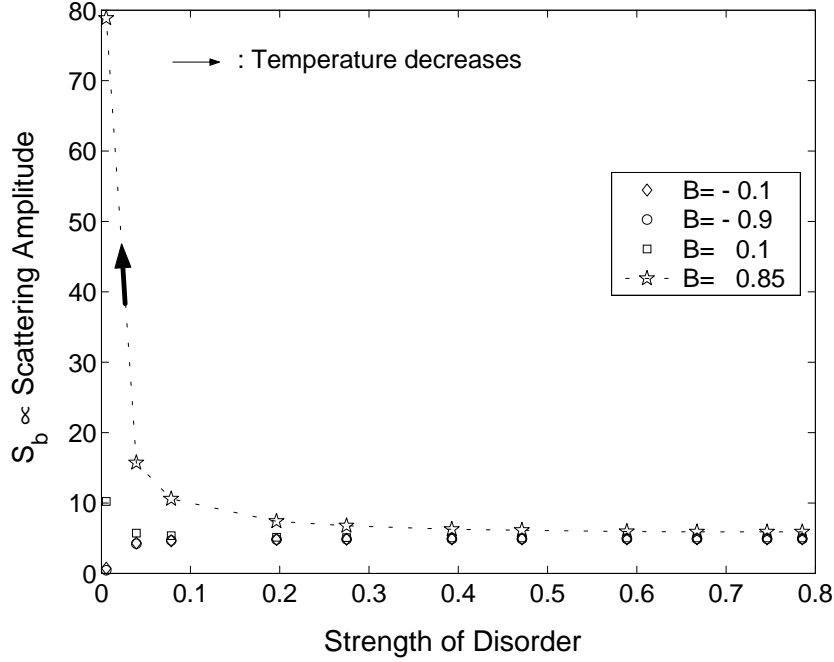


Fig. 3 Possible phase diagram for non-Fermi gases w.r.t. the disorder and the scattering amplitude  $S_b$ .  $S_b \propto BK_n$  and  $K_n \propto$  the mean free path. Note that the resistivity is proportional to the strength of disorder in 2D [5-6]. Here, once the temperature is lowered down the resistivity firstly increases and then decreases.

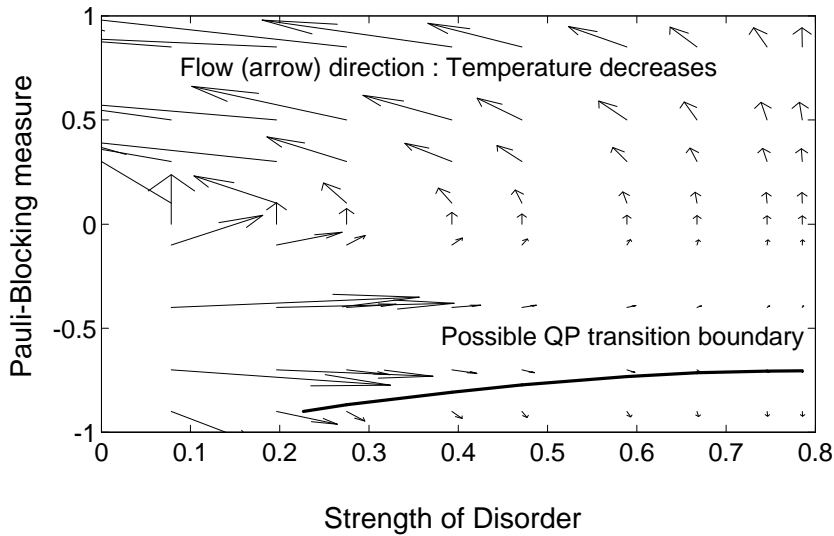


Fig. 4 Possible flow pattern for  $S_b$  w.r.t. the disorder and Pauli-blocking measure ( $B$ ).  $S_b \propto BK_n$  and  $K_n \propto$  the mean free path. Note that the resistivity is proportional to the disorder [5-6] in 2D. Each continuous flow represents the behavior when  $T$  is decreased, and different paths represent different values of Pauli-blocking measure. (cf Fig. 4 in [5])



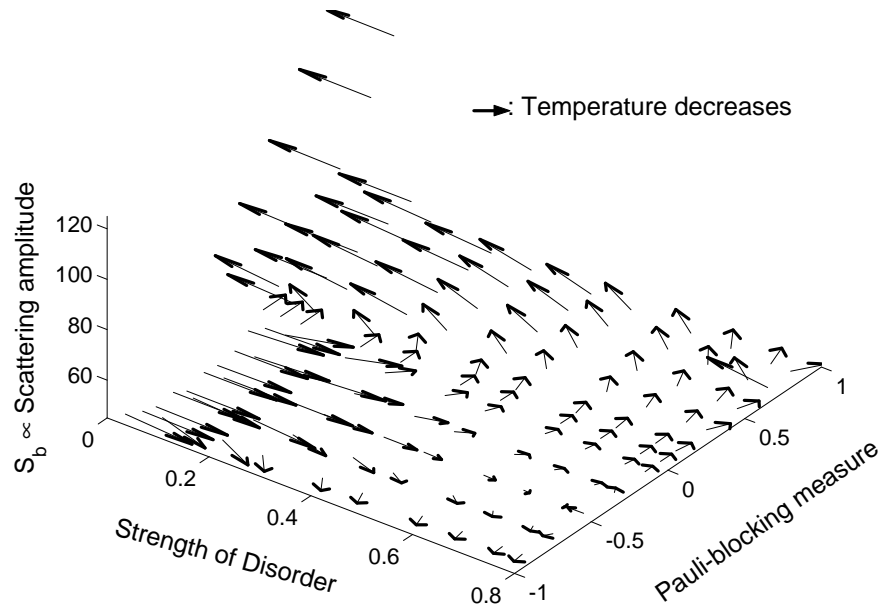


Fig. 5 Possible scattering amplitude ( $S_b$ ) vs. disorder and Pauli-blocking measure curves.  $S_b \propto BK_n$ , and  $K_n \propto$  the mean free path. Note that the resistivity is proportional to the strength of disorder in 2D [6]. Here, the flow (arrow) direction means that the temperature is decreasing. These results resemble qualitatively those proposed by Abrahams in [5-6].